HHS Public Access

Author manuscript

Nat Cell Biol. Author manuscript; available in PMC 2012 May 01.

Published in final edited form as:

Nat Cell Biol. ; 13(11): 1361–1367. doi:10.1038/ncb2354.

Microtubules induce self-organization of polarized PAR domains in *C. elegans* zygotes

Fumio Motegi, **Seth Zonies**, **Yingsong Hao**, **Adrian A. Cuenca**, **Erik Griffin**, and **Geraldine Seydoux**

Department of Molecular Biology and Genetics, Howard Hughes Medical Institute, Center for Cell Dynamics, Johns Hopkins University School of Medicine, 725 N. Wolfe St., PCTB 706, Baltimore, MD 21205, USA

Abstract

A hallmark of polarized cells is the segregation of the PAR polarity regulators into asymmetric domains at the cell cortex[1, 2]. Antagonistic interactions involving two conserved kinases, atypical protein kinase C (aPKC) and PAR-1, have been implicated in polarity maintenance[1, 2], but the mechanisms that initiate the formation of asymmetric PAR domains are not understood. Here, we describe one pathway used by the sperm-donated centrosome to polarize the PAR proteins in *Caenorhabditis elegans* zygotes. Before polarization, cortical aPKC excludes PAR-1 kinase and its binding partner PAR-2 by phosphorylation. During symmetry breaking, microtubules nucleated by the centrosome locally protect PAR-2 from phosphorylation by aPKC, allowing PAR-2 and PAR-1 to access the cortex nearest the centrosome. Cortical PAR-1 phosphorylates PAR-3, causing the PAR-3/aPKC complex to leave the cortex. Our findings illustrate how microtubules, independent of actin dynamics, stimulate the self-organization of PAR proteins by providing local protection against a global barrier imposed by aPKC.

Newly fertilized *C. elegans* zygotes have no predetermined anterior/posterior polarity. Before symmetry breaking, the PDZ domain proteins PAR-3 and PAR-6 and the kinase aPKC/PKC-3 (“anterior PARs”) are uniformly at the cell cortex, and maintain the kinase PAR-1 and the RING protein PAR-2 (“posterior PARs”) in the cytoplasm. During symmetry breaking, the sperm centrosome (or microtubule-organizing center, MTOC) contacts the cortex[1, 2] eliciting two changes: actomyosin flows directed away from the MTOC[3], and recruitment of PAR-2 to the cortex nearest the MTOC (Fig. 1a)[4]. Actomyosin flows and PAR-2 function in parallel to displace anterior PARs from the cortex, allowing PAR-1 to also load on the posterior cortex. After cortical flows cease, PAR-2 becomes essential to prevent anterior PARs from returning to the posterior cortex (polarity maintenance)[3, 5]. In this study, we investigate how the MTOC recruits PAR-2 to the cortex, and how PAR-2 in turn displaces anterior PARs.

AUTHOR CONTRIBUTIONS: F.M. and G.S. designed the study and wrote the manuscript. S.Z. performed experiments show in Fig. 3b and Supplementary Fig. S5b, Y.H. A.A.C. and E.G. performed experiments show in Supplementary Fig. S8c,d, and F.M. performed all other experiments.

We first examined PAR-2 dynamics in fixed zygotes depleted of the myosin regulatory light chain MLC-4[6] (Fig. 1 and Supplementary Fig. S1a). *mlc-4(RNAi)* zygotes do not develop cortical flows and depend solely on PAR-2 for symmetry breaking[4]. Before symmetry breaking, PAR-2 was in the cytoplasm and weakly enriched at the MTOC core (Fig. 1b and Supplementary Fig. S1a). During symmetry breaking, PAR-2 appeared on the cortex. In 21 of 28 (endogenous PAR-2) and 25 of 30 (GFP::PAR-2) zygotes fixed at this stage, PAR-2 was unevenly distributed on the cortex, with the highest levels at the microtubule-dense core of the MTOC (Fig. 1c and Supplementary Fig. S1a). The plasma membrane marker mCherry::PH^{PLC} was uniformly distributed at this stage (Supplementary Fig. S1a). After symmetry breaking, PAR-2 distribution on the cortex became more uniform (Fig. 1d) and the PAR-2 domain expanded to reach 32 +/− 5.2% of the embryo's circumference (Fig. 1f). Live imaging confirmed that the PAR-2 domain correlates with the site of MTOC/cortex contact (Supplementary Fig. S1c). Treatments that interfere with microtubule nucleation, yielded zygotes that formed no cortical GFP::PAR-2 domains, or domains that were significantly smaller (12.1 +/− 5.1%) and appeared later than controls (Fig. 1e,f and Supplementary Fig. S1d). We conclude that, in the absence of cortical flows, PAR-2 loading depends on microtubules and correlates spatially and temporally with MTOC/cortex contact.

Enrichment of PAR-2 on the MTOC core during symmetry breaking suggested that PAR-2 has microtubule-binding activity. We found that recombinant PAR-2 could be pelleted with, but not without, microtubules by high-speed centrifugation (Kd apparent: 1.19 μM, Fig. 2b and Supplementary Fig. S2). Visualization of recombinant GFP::PAR-2 mixed with rhodamine-labeled microtubules confirmed that PAR-2 binds microtubules *in vitro* (Fig. 2c). Deletion analysis identified three microtubule-binding regions in PAR-2 (Fig. 2a and Supplementary Fig. S3a). A fusion [GFP::PAR-2(1–221)] containing the first microtubule-binding region but lacking the cortical localization domain localized to spindles *in vivo* (Supplementary Fig. S3a). Full-length GFP::PAR-2 also localized to spindles, but only in zygotes treated with the microtubule-stabilizing drug taxol (Supplementary Fig. S3b). Mutagenesis of basic residues conserved in *C. briggsae* and *C. remanei* PAR-2 yielded two mutations (R163A and R183-5A) that significantly reduced microtubule binding *in vitro* (Fig. 2a–c and Supplementary Figs. S2 and S4). R183-5A also interfered with the localization of GFP::PAR-2(1–221) to spindles (Supplementary Fig. S3a), and with the localization of full-length PAR-2 to taxol-stabilized spindles (Supplementary Fig. S3b), and to the MTOC at symmetry breaking (Supplementary Fig. S1b). We conclude that the first microtubule-binding domain of PAR-2 is necessary and sufficient for interactions with microtubules *in vitro* and *in vivo*, and that microtubule binding is required to enrich PAR-2 on the MTOC core during symmetry breaking.

To determine the function of microtubule binding, we expressed GFP::PAR-2(R163A) and GFP::PAR-2(R183-5A) from RNAi-resistant transgenes in *mlc-4(RNAi)* zygotes depleted of endogenous PAR-2 (see Methods). For positive controls, we used wild-type GFP::PAR-2 and a mutation (K162A) in the first microtubule-binding domain that does not affect microtubule-binding affinity *in vitro* (Fig. 2b and Supplementary Fig. S2). All fusions were expressed at comparable levels (Supplementary Fig. S5a). Whereas GFP::PAR-2 and GFP::PAR-2(K162A) localized to the posterior cortex, GFP::PAR-2(R163A) and

GFP::PAR-2(R183-5A) remained in the cytoplasm in the majority of zygotes (Fig. 3a and Supplementary Table 1). We obtained identical results under three other conditions that eliminate MTOC-induced cortical flows; *ect-2(ax751)*[4], *mat-1(ax227)*[7], and *spd-5(RNAi)*[8] (Fig. 3a and Supplementary Table 1). Localization to the cortex was restored by reducing PKC-3 by RNAi or by eliminating the PKC-3 phosphorylation sites in PAR-2 (Fig. 3a and Supplementary Table 1). GFP::PAR-2 and GFP::PAR-2(R183-5A) exhibited identical cortical dynamics in *pkc-3(RNAi)* zygotes as revealed by fluorescence-recovery after photobleaching (FRAP)(Fig. 3b and Supplementary Fig. S5b). GFP::PAR-2(R163A) and GFP::PAR-2(R183-5A) localized to the posterior cortex in *mlc-4(+)* embryos (where PKC-3 is mobilized by flows) (Fig. 3a) and could rescue the embryonic lethality of *par-2(RNAi)* and/or *par-2(lw32)* zygotes to the same extent as wild-type GFP::PAR-2 (Supplementary Table 2). We conclude that microtubule binding is essential for symmetry breaking but not for polarity maintenance, or for PAR-2 to associate with the cortex in the absence of PKC-3.

How does microtubule binding facilitate PAR-2 cortical loading at symmetry breaking? The microtubule-binding regions of PAR-2 contain several PKC-3 phosphorylation sites (Fig. 2a), raising the possibility that microtubule binding protects PAR-2 from phosphorylation by PKC-3. Consistent with this possibility, addition of microtubules inhibited the phosphorylation of PAR-2 by human aPKC *in vitro* (Fig. 2d and Supplementary Fig. S6a). Inhibition was not observed in the presence of nocodazole (Supplementary Fig. S6b), or when the PAR-2 microtubule-binding mutants (R163A and R183-5A) were used as substrates (Fig. 2d and Supplementary Fig. S6a). Consistent with microtubules acting as competitive inhibitors, 0.8 μM polymerized tubulin was sufficient to increase the K_m by 65% without affecting the V_{max} of the aPKC kinase reaction (Supplementary Fig. S6c). The average intracellular tubulin concentration has been estimated at ~20 μM[9] and should be even higher at the MTOC core, consistent with the possibility that microtubules protect PAR-2 from PKC-3 at symmetry breaking.

To test this hypothesis further, we developed an *in vitro* microtubule/PKC-3 competition assay in the presence of a “cortex mimic”. Interactions with plasma membrane phospholipids have been implicated in the localization of PAR-1 and PAR-3 homologs to the cortex[10, 11]. Using a protein-lipid binding assay, we found that PAR-2 interacts with phospholipids including phosphoinositides (Fig. 2e,f and Supplementary Fig. S7). Phosphorylation by aPKC, or phosphomimetic mutations in the PKC-3 sites, interfered with PAR-2 binding to lipids (Fig. 2e,f and Supplementary Fig. S7), as they interfere with PAR-2 cortical localization *in vivo*[12]. Remarkably, preincubation with 1.5 μM polymerized tubulin rescued PAR-2’s ability to bind to lipids in the presence of aPKC (Fig. 2f and Supplementary Fig. S7c). Microtubules did not restore lipid binding to PAR-2(R183-5A) (Fig. 2f and Supplementary Fig. S7c), even though this mutant could bind lipids as efficiently as wild-type PAR-2 in the absence of aPKC (Fig. 2e and Supplementary Fig. S7a,b). We conclude that binding to microtubules is sufficient to protect PAR-2 from aPKC/PKC-3 and retain binding to plasma membrane lipids.

After reaching the cortex, PAR-2 becomes partially resistant to exclusion by PKC-3, and this resistance depends on the PAR-2 RING domain[12]. FRAP analyses revealed faster cortical dynamics for the RING mutant GFP::PAR-2(C56S) compared to GFP::PAR-2 and

GFP::PAR-2(R183-5A) (Fig. 3b and Supplementary Fig. S5b). GFP::PAR-2(C56S) was enriched on the MTOC at the time of MTOC/cortex contact in most *mlc-4(RNAi)* zygotes (14 of 25), but did not form a posterior cortical domain (Fig. 3c and Supplementary Fig. S1b). Endogenous PAR-2 could rescue the cortical localization of both GFP::PAR-2(C56S) and GFP::PAR-2(R183-5A) in *mlc-4(RNAi)* zygotes (Fig. 3c). These results indicate that cortical PAR-2 is stabilized at the cortex by its RING domain, and recruits additional PAR-2 molecules from the cytoplasm independent of microtubule binding.

By pronuclear meeting, PAR-3 and PKC-3 were excluded from the PAR-2 domain (Fig. 4a and Supplementary Table 3). This exclusion was dependent on PAR-1 (Fig. 4a and Supplementary Table 3). PAR-1 co-localized with PAR-2 on the posterior cortex in *mlc-4(RNAi)* zygotes expressing wild-type GFP::PAR-2, but not in zygotes expressing GFP::PAR-2(R183-5A), where PAR-2 does not load and PAR-3 and PKC-3 are not excluded (Fig. 4a and Supplementary Table 3). In *Drosophila* oocytes, PAR-1 phosphorylates PAR-3, causing PAR-3 to lose its cortical association[13]. *In vitro* kinase assays confirmed that *C. elegans* PAR-1 can phosphorylate PAR-3 (Supplementary Fig. S8a,b). Furthermore, we found that PAR-3 and PKC-3 were not excluded in zygotes where PAR-1 lacked kinase activity[14] or its cortical localization domain[15], or in zygotes expressing a PAR-3 fusion missing the PAR-1 phosphorylation sites[16] (Fig. 4a and Supplementary Table 3). We conclude that recruitment of PAR-1 to the PAR-2 domain leads to exclusion of the PAR-3/PKC-3 complex, likely by direct phosphorylation of PAR-3 by PAR-1.

How does PAR-2 recruit PAR-1? In mammalian cells, PAR-1 cortical localization depends on a C-terminal domain that contains a conserved aPKC phosphorylation site required for cortical exclusion by aPKC[17]. We confirmed that the corresponding domain of *C. elegans* PAR-1 (965–1192 aa) is necessary and sufficient to target PAR-1 to the cortex (Supplementary Fig. S8c), and that the conserved aPKC site T983 can be phosphorylated by aPKC *in vitro* (Supplementary Fig. S8d) and is required to exclude PAR-1 from PKC-3(+) cortices *in vivo* (Supplementary Fig. S8c). Remarkably, we found that GFP::PAR-1(965–1193 aa) and PAR-1(*it51*), which cannot exclude PAR-3 and PKC-3, were still able to localize with PAR-2 on the posterior cortex in *mlc-4(RNAi)* zygotes (Fig. 4a and Supplementary Table 3), indicating that PAR-2 can recruit PAR-1 to cortices also occupied by PKC-3. To determine if PAR-1 and PAR-2 interact, we first immunoprecipitated GFP::PAR-1 and GFP::PAR-2 from worm extracts. We detected endogenous PAR-2 in GFP::PAR-1 immunoprecipitates and endogenous PAR-1 in GFP::PAR-2 immunoprecipitates, indicating that at least a subset of PAR-2 and PAR-1 molecules are in a complex (Fig. 4b). Using purified recombinant proteins, we found that PAR-1 and PAR-2 interact directly, and that the PAR-1 C-terminus is sufficient for the interaction (Supplementary Fig. S8e). We conclude that PAR-2 recruits PAR-1 to the cortex, via a direct interaction involving the PAR-1 C-terminal domain.

In wild-type embryos, depletion of tubulin delays symmetry breaking[18], raising the possibility that microtubule-dependent loading of PAR-2 contributes to symmetry breaking even in the presence of flows. Consistent with this possibility, at symmetry breaking, GFP::PAR-2(R183-5A) zygotes showed either uniform PAR-3 and no PAR-2 at the cortex (2 of 12), or asymmetric PAR-3 and no (5 of 12) or low PAR-2 (5 of 12). In contrast, 9 of 10

zygotes expressing wild-type GFP::PAR-2 already had complementary PAR-2/PAR-3 domains at this stage (Fig. 5a). Live imaging experiments revealed that GFP::PAR-2(R183-5A) loads on the posterior cortex 29.0 +/−11.2 seconds later than GFP::PAR-2 (Fig. 5b). After this initial delay, GFP::PAR-2(R183-5A) cortical levels increased rapidly and were indistinguishable from GFP::PAR-2 levels by mitosis (Fig. 5a,b), and all zygotes fixed at this stage excluded PAR-3 from the GFP::PAR-2 domain (Fig. 5a). We conclude that, in wild-type embryos, microtubule binding by PAR-2 contributes to the fast kinetics of PAR-2 loading/PAR-3 clearing, but is not essential after cortical flows displace anterior PARs.

Our observations suggest a simple model for polarization of the *C. elegans* zygote (Fig. 5c). When the MTOC contacts the cortex, the high density of microtubules transiently protects PAR-2 from phosphorylation by PKC-3, allowing a few molecules of unphosphorylated PAR-2 to interact productively with the cortex. Cortical PAR-2, stabilized by its RING domain, recruits PAR-1 as well as additional PAR-2 molecules ("PAR-2 feedback loop"), allowing the PAR-2/PAR-1 domain to expand beyond the site of MTOC/cortex contact. PAR-1 phosphorylates PAR-3, causing the PAR-3/PKC-3 complex to leave the cortex. The anterior PARs are also displaced by cortical flows triggered by the MTOC. Both symmetry-breaking functions of the MTOC (induction of cortical flows and protection of PAR-2 from PKC-3) are transient and depend on the PAR-2 feedback loop and PAR-1 for PAR domain maintenance (also see[12]).

This model clarifies several observations in the literature. First, although some studies support a role for microtubules in symmetry breaking[7, 18], others have suggested that microtubules are not required[19, 20]. Our findings demonstrate a role for microtubules to load PAR-2 at the earliest stage of symmetry breaking, but leave open the possibility that the MTOC uses a second, microtubule-independent cue to initiate cortical flows[21]. Our model also explains why PAR-2 is not essential to exclude anterior PARs in *par-6/+* zygotes[22, 23] or zygotes that overexpress LGL-1, which, like PAR-1, antagonizes the cortical localization of anterior PARs[24, 25]. We suggest that the primary function of the PAR-2 feedback loop is to maintain sufficient PAR-1 on the posterior cortex to ensure permanent exclusion of anterior PARs. This function may not be needed in embryos where cortical levels of anterior PARs are already biased by flows and further reduced by mutation or LGL-1 overexpression. A remaining question is what prevents the PAR-2 domain from spreading to the entire cortex. Anterior and posterior PARs exchange with the cytoplasm and diffuse freely across the PAR boundary[26]. One possibility, therefore, is that as the anterior PARs become restricted to a smaller region of the cortex, the concentration of PKC-3 at the boundary reaches a threshold sufficient to block further PAR-2 spreading.

The PAR system has been implicated in the polarization of several cell types, including some that do not undergo cortical flows[27]. Our findings illustrate how the self-organizing properties of the PAR network are sufficient to polarize a cell in the absence of long-range actin dynamics. In principle, any localized cue that favors the binding of one class of PARs with the cortex will be sufficient to initiate a cascade of self-organizing interactions within the network. We suggest that cortical flows, while non-essential, contribute to the polarization process by increasing the robustness of the response. Cortical flows may also

serve to align PAR asymmetry with the cell's intrinsic geometry, as PAR domains are often miss-aligned with respect to the long axis of *mlc-4(RNAi)* zygotes (Fig. 4a and reference[4]).

Microtubules have been proposed to polarize cells by transporting polarity regulators to specific regions of the cell (reviewed in reference[28]). Our findings identify another way microtubules break symmetry: by protecting polarity regulators from cortical exclusion by aPKC.

Supplementary Material

Refer to Web version on PubMed Central for supplementary material.

Acknowledgments

This study was supported by the Japan Society for the Promotion of Science ([F.M.]), the American Cancer Society (PF-08-158-01 [E.G.]), and the National Institute of Health (R01HD37047 [G.S.]). G.S. is an investigator of the Howard Hughes Medical Institute. We thank J. Ahringer, A. Audhya, L. Boyd, A. Desai, P. Gonczy, M. Gotta, R. Green, C. Hoege, K. Kemphues, Y. Nishimura, K. F. O'Connell, K. Oegema, L. S. Rose, A. Sugimoto, C. M. Waterman, H. Zaher, and the Caenorhabditis Genetic Center for reagents and expertise.

References

1. Goldstein B, Macara I. The PAR proteins: fundamental players in animal cell polarization. Dev Cell. 2007; 13:609–622. [PubMed: 17981131]
2. St Johnston D, Ahringer J. Cell polarity in eggs and epithelia: parallels and diversity. Cell. 2010; 141:757–774. [PubMed: 20510924]
3. Munro E, Nance J, Priess JR. Cortical flows powered by asymmetrical contraction transport PAR proteins to establish and maintain anterior-posterior polarity in the early C. elegans embryo. Dev Cell. 2004; 7:413–424. [PubMed: 15363415]
4. Zonies S, Motegi F, Hao Y, Seydoux G. Symmetry breaking and polarization of the C. elegans zygote by the polarity protein PAR-2. Development. 2010; 137:1669–1677. [PubMed: 20392744]
5. Cuenca AA, Schetter A, Aceto D, Kemphues K, Seydoux G. Polarization of the C. elegans zygote proceeds via distinct establishment and maintenance phases. Development. 2003; 130:1255–1265. [PubMed: 12588843]
6. Shelton C, Carter J, Ellis G, Bowerman B. The nonmuscle myosin regulatory light chain gene mlc-4 is required for cytokinesis, anterior-posterior polarity, and body morphology during Caenorhabditis elegans embryogenesis. J Cell Biol. 1999; 146:439–451. [PubMed: 10427096]
7. Wallenfang MR, Seydoux G. Polarization of the anterior-posterior axis of C. elegans is a microtubule-directed process. Nature. 2000; 408:89–92. [PubMed: 11081513]
8. Hamill DR, Severson AF, Carter JC, Bowerman B. Centrosome maturation and mitotic spindle assembly in C. elegans require SPD-5, a protein with multiple coiled-coil domains. Dev Cell. 2002; 3:673–684. [PubMed: 12431374]
9. Hiller G, Weber K. Radioimmunoassay for tubulin: a quantitative comparison of the tubulin content of different established tissue culture cells and tissues. Cell. 1978; 14:795–804. [PubMed: 688394]
10. Moravcevic K, et al. Kinase associated-1 domains drive MARK/PAR1 kinases to membrane targets by binding acidic phospholipids. Cell. 2010; 143:966–977. [PubMed: 21145462]
11. Wu H, et al. PDZ domains of Par-3 as potential phosphoinositide signaling integrators. Mol Cell. 2007; 28:886–898. [PubMed: 18082612]
12. Hao Y, Boyd L, Seydoux G. Stabilization of cell polarity by the C. elegans RING protein PAR-2. Dev Cell. 2006; 10:199–208. [PubMed: 16459299]
13. Benton R, St Johnston D. Drosophila PAR-1 and 14-3-3 inhibit Bazooka/PAR-3 to establish complementary cortical domains in polarized cells. Cell. 2003; 115:691–704. [PubMed: 14675534]

14. Guo S, Kemphues K. par-1, a gene required for establishing polarity in C. elegans embryos, encodes a putative Ser/Thr kinase that is asymmetrically distributed. Cell. 1995; 81:611–620. [PubMed: 7758115]
15. Griffin E, Odde E, Seydoux G. Regulation of the MEX-5 gradient by a spatially segregated kinase/phosphatase cycle. Cell. in press.
16. Li B, Kim H, Beers M, Kemphues K. Different domains of C. elegans PAR-3 are required at different times in development. Dev Biol. 2010; 344:745–757. [PubMed: 20678977]
17. Matenia D, Mandelkow EM. The tau of MARK: a polarized view of the cytoskeleton. Trends Biochem Sci. 2009; 34:332–342. [PubMed: 19559622]
18. Tsai MC, Ahringer J. Microtubules are involved in anterior-posterior axis formation in C. elegans embryos. J Cell Biol. 2007; 179:397–402. [PubMed: 17967950]
19. Cowan CR, Hyman AA. Centrosomes direct cell polarity independently of microtubule assembly in C. elegans embryos. Nature. 2004; 431:92–96. [PubMed: 15343338]
20. Sonneville R, Gonczy P. zyg-11 and cul-2 regulate progression through meiosis II and polarity establishment in C. elegans. Development. 2004; 131:3527–3543. [PubMed: 15215208]
21. Jenkins N, Saam JR, Mango SE. CYK-4/GAP provides a localized cue to initiate anteroposterior polarity upon fertilization. Science. 2006; 313:1298–1301. [PubMed: 16873611]
22. Watts J, et al. par-6, a gene involved in the establishment of asymmetry in early C. elegans embryos, mediates the asymmetric localization of PAR-3. Development. 1996; 122:3133–3140. [PubMed: 8898226]
23. Labbé JC, Pacquelet A, Marty T, Gotta M. A genomewide screen for suppressors of par-2 uncovers potential regulators of PAR protein-dependent cell polarity in Caenorhabditis elegans. Genetics. 2006; 174:285–295. [PubMed: 16816419]
24. Hoege C, et al. LGL can partition the cortex of one-cell Caenorhabditis elegans embryos into two domains. Curr Biol. 2010; 20:1296–1303. [PubMed: 20579886]
25. Beatty A, Morton D, Kemphues K. The C. elegans homolog of Drosophila Lethal giant larvae functions redundantly with PAR-2 to maintain polarity in the early embryo. Development. 2010
26. Goehring NW, Hoege C, Grill SW, Hyman AA. PAR proteins diffuse freely across the anterior-posterior boundary in polarized C. elegans embryos. J Cell Biol. 2011; 193:583–594. [PubMed: 21518794]
27. Doerflinger H, et al. Bazooka is required for polarisation of the Drosophila anterior-posterior axis. Development. 2010; 137:1765–1773. [PubMed: 20430751]
28. Siegrist SE, Doe CQ. Microtubule-induced cortical cell polarity. Genes Dev. 2007; 21:483–496. [PubMed: 17344411]
29. Morita K, Hirono K, Han M. The Caenorhabditis elegans ect-2 RhoGEF gene regulates cytokinesis and migration of epidermal P cells. EMBO Rep. 2005; 6:1163–1168. [PubMed: 16170304]
30. Kachur T, Audhya A, Pilgrim D. UNC-45 is required for NMY-2 contractile function in early embryonic polarity establishment and germline cellularization in C. elegans. Dev Biol. 2008; 314:287–299. [PubMed: 18190904]
31. Etemad-Moghadam B, Guo S, Kemphues K. Asymmetrically distributed PAR-3 protein contributes to cell polarity and spindle alignment in early C. elegans embryos. Cell. 1995; 83:743–752. [PubMed: 8521491]
32. Merritt C, Seydoux G. Transgenic solutions for the germline. WormBook. 2010:1–21. [PubMed: 20169625]
33. Praitis V, Casey E, Collar D, Austin J. Creation of low-copy integrated transgenic lines in Caenorhabditis elegans. Genetics. 2001; 157:1217–1226. [PubMed: 11238406]
34. Maeda I, Kohara Y, Yamamoto M, Sugimoto A. Large-scale analysis of gene function in Caenorhabditis elegans by high-throughput RNAi. Curr Biol. 2001; 11:171–176. [PubMed: 11231151]
35. Kamath R, et al. Systematic functional analysis of the Caenorhabditis elegans genome using RNAi. Nature. 2003; 421:231–237. [PubMed: 12529635]
36. Hannak E, Kirkham M, Hyman AA, Oegema K. Aurora-A kinase is required for centrosome maturation in Caenorhabditis elegans. J Cell Biol. 2001; 155:1109–1116. [PubMed: 11748251]

37. Dong Y, Bogdanova A, Habermann B, Zachariae W, Ahringer J. Identification of the C. elegans anaphase promoting complex subunit Cdc26 by phenotypic profiling and functional rescue in yeast. BMC Dev Biol. 2007; 7:19. [PubMed: 17374146]

38. Nance J, Munro E, Priess JC. elegans PAR-3 and PAR-6 are required for apicobasal asymmetries associated with cell adhesion and gastrulation. Development. 2003; 130:5339–5350. [PubMed: 13129846]

39. Aono S, Legouis R, Hoose W, Kemphues K. PAR-3 is required for epithelial cell polarity in the distal spermatheca of C. elegans. Development. 2004; 131:2865–2874. [PubMed: 15151982]

40. Goode B, Feinstein S. Identification of a novel microtubule binding and assembly domain in the developmentally regulated inter-repeat region of tau. J Cell Biol. 1994; 124:769–782. [PubMed: 8120098]

41. Nesić D, et al. Helicobacter pylori CagA inhibits PAR1-MARK family kinases by mimicking host substrates. Nat Struct Mol Biol. 2010; 17:130–132. [PubMed: 19966800]

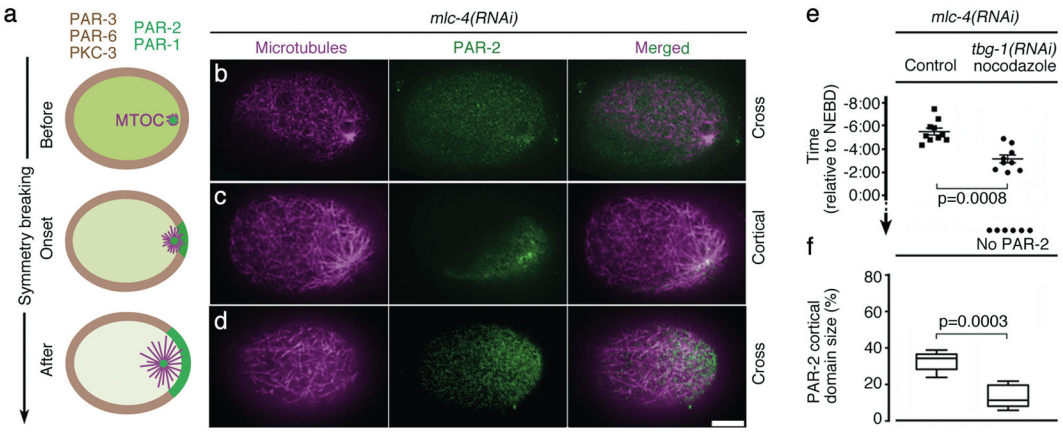

Figure 1. PAR-2 dynamics at symmetry breaking

(**a**) Embryo schematics showing the distribution of PAR-1 and PAR-2 (green), anterior PARs (brown), and MTOC/microtubules (magenta). Zygotes are oriented with posterior to the right in this and all figures.

(**b–d**) Confocal images of fixed *mlc-4(RNAi)* zygotes stained for tubulin (magenta) and PAR-2 (green). Note that **b** shows a cross-section as in the schematics in **a**, whereas **c** and **d** show superficial cortical sections. Scale bar, 10 μm.

(**e**) Graph showing the timing of GFP::PAR-2 appearance on the posterior cortex in live *mlc-4(RNAi)* zygotes relative to nuclear envelope breakdown (NEBD). Each dot represents an individual zygote. “no PAR-2” refers to zygotes where PAR-2 never loaded on the cortex. “*tbg-1(RNAi)* nocodazole” refers to zygotes depleted for gamma-tubulin and treated with nocodazole. Error bars represent standard deviation from 10 control zygotes and 9 *tbg-1(RNAi)* nocodazole zygotes with a cortical GFP::PAR-2 domain.

(**f**) Graphs showing size of GFP::PAR-2 domain scored at NEBD. Error bars represent standard deviation in zygotes with a cortical GFP::PAR-2 domain as in **e**. See Supplementary Fig. S1d for images of zygotes used to compile data in **e** and **f**.

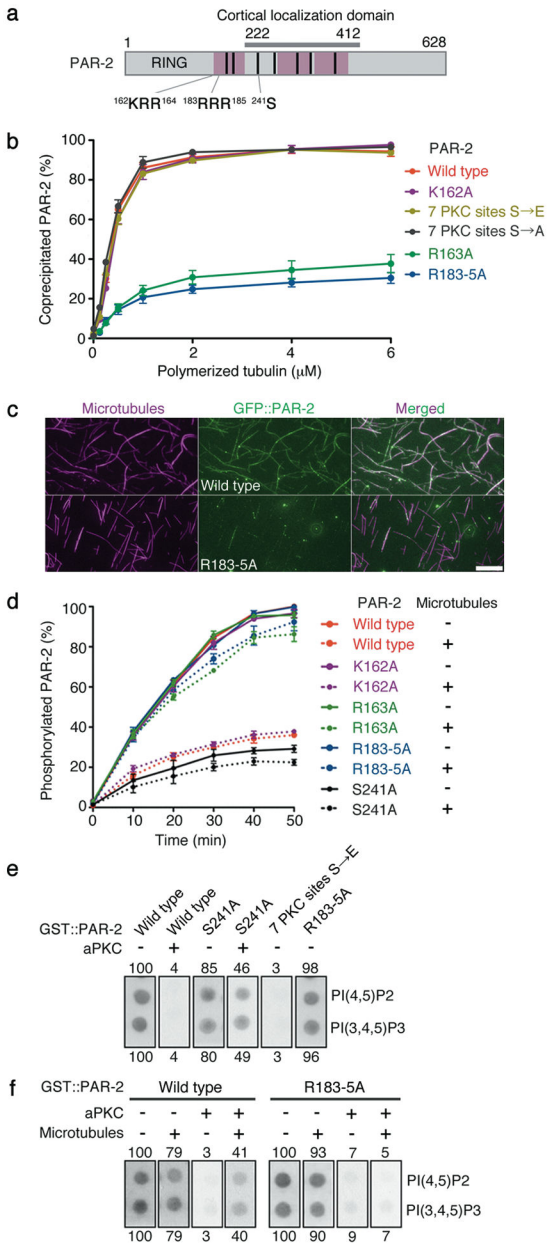

Figure 2. Microtubule binding protects PAR-2 from aPKC phosphorylation and allows PAR-2 to interact with phospholipids in the presence of aPKC

(**a**) PAR-2 schematic. Pink boxes are regions that contribute to microtubule binding *in vitro* (see Supplementary Fig. S3a). Cortical localization domain is the region sufficient for localization to the posterior cortex in the presence of endogenous PAR-2 (reference[12] and F. Motegi, unpublished). Black bars indicate seven potential PKC-3 phosphorylation sites[12]. S241 is required for maximal phosphorylation *in vitro* by aPKC (Fig. 2d) and for cortical exclusion *in vivo* (Fig. 3a). ^{162}KRR^{164} is the basic cluster mutated in the single substitution mutants K162A and R163A, and ^{183}RRR^{185} is the basic cluster mutated in the triple substitution mutant R183-5A.

(**b**) Graph depicting the percent recombinant PAR-2 that co-sedimented with microtubules. Error bars represent standard deviation in three independent experiments.
(**c**) Photomicrographs of recombinant GFP::PAR-2 mixed with rhodamine-labeled microtubules and spread on slides. GFP::PAR-2(R183-5A) does not decorate microtubules as efficiently as wild-type GFP::PAR-2. Scale bar, 5 μm.
(**d**) Graph depicting the percent phosphorylated PAR-2 with respect to time since start of incubation with aPKC kinase in the presence (dotted lines) or absence (solid lines) of microtubules. PAR-2 phosphorylation was monitored by ^{32}P-ATP incorporation. Error bars represent standard deviation in three independent experiments.
(**e**) Phosphorylation by aPKC inhibits PAR-2 from binding to phospholipids. GST::PAR-2 fusions pre-treated with or without aPKC were incubated with lipid strips and detected using an anti-GST antibody. 50 pmol PI(4,5)P2 and PI(3,4,5)P3 spots are shown (see Supplementary Fig. S7b for the full dilution series). Numbers represent % binding normalized to wild type (100%). S241 is one of 7 predicted aPKC sites. 7PKCsitesS→E is a phosphomimic mutant for all seven sites.
(**f**) Binding to microtubules is sufficient to protect PAR-2 from aPKC and retain binding to phospholipids. Same as in **e**, but GST::PAR-2 fusions were incubated with microtubules before incubation with aPKC. See Supplementary Fig. S7c for the full dilution series.

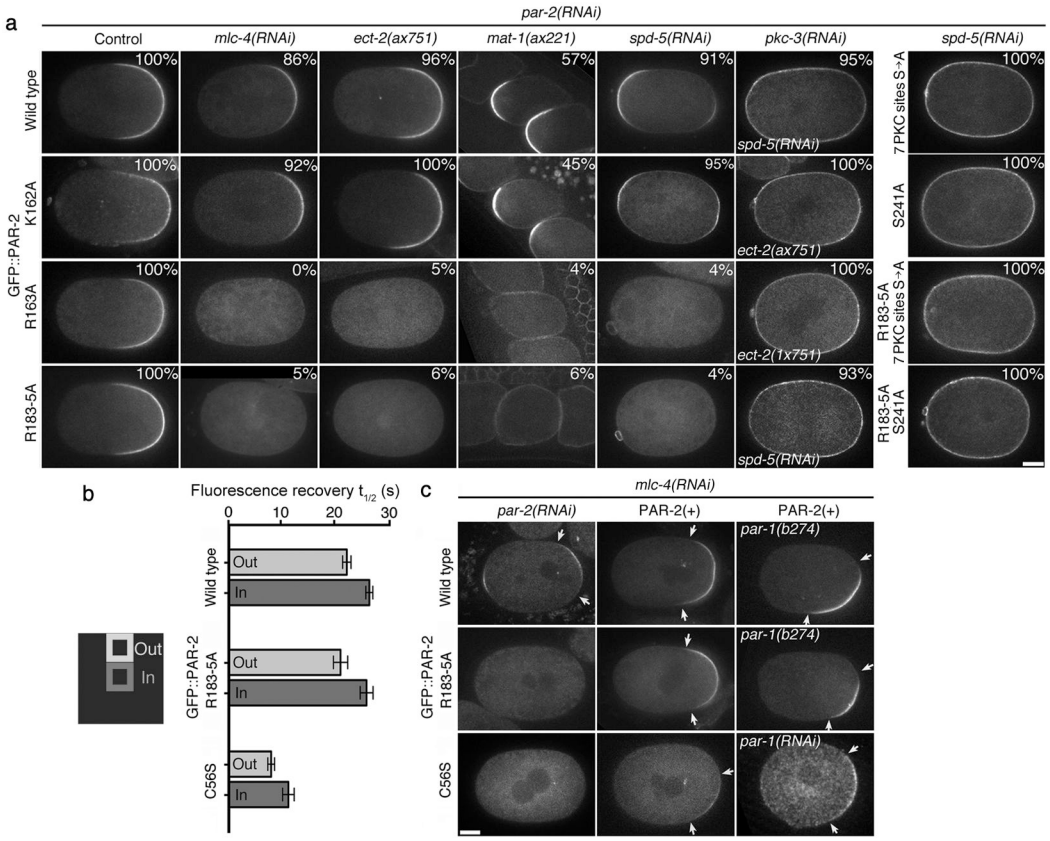

Figure 3. Microtubule binding is required for PAR-2 to localize to the cortex in the absence of cortical flows

(**a**) Live zygotes expressing the indicated GFP::PAR-2 fusions: wild type and K162A bind microtubules, R163A and R183-5A do not. % indicate zygotes with cortical PAR-2, numbers are presented in Supplementary Table 1. ECT-2 is the GEF for the small GTPase RHO-1[29]. *ect-2(ax751)* lack MTOC-induced cortical flows, but develop PAR-2-dependent cortical flows during mitosis[4]. MAT-1 is a subunit of the anaphase-promoting complex. *mat-1(ax227)* zygotes arrest in meiosis and become transiently polarized without cortical flows under the influence of the acentriolar meiotic spindle[7]. SPD-5 is a MTOC component required for PCM assembly[8]. *spd-5(RNAi)* zygotes localize GFP::PAR-2 to both the anterior and posterior cortex under the influence of the meiotic spindle remnant (anterior) and the slow maturing MTOC (posterior)[18]. RNAi depletion of PKC-3 or mutations in the PKC phosphorylation sites (either 7 PKC sites S→A or S241A) causes all fusions to localize uniformly to the cortex. Scale bar, 10 μm.

(**b**) Fluorescence Recovery After Photobleaching was performed on the cortex of *pkc-3(RNAi)* zygotes expressing the indicated GFP::PAR-2 fusions. Graph shows the average recovery half time (t½) from five separate zygotes. Error bars represent standard deviation. Fluorescence recovery was faster at the boundary (Out) than at the center (In) of the bleached area, suggesting that at least some of the recovery is due to lateral diffusion of cortical GFP::PAR-2 as shown in reference[26]. See supplementary Fig. S5b for representative recovery curves.

(**c**) Cortical PAR-2 stimulates its own recruitment to the cortex. Live zygotes expressing the indicated GFP::PAR-2 fusions. Arrows point to the boundaries of the cortical GFP::PAR-2 domain. Scale bar, 10 μm. In *mlc-4(RNAi);par-2(RNAi)* zygotes, wild-type PAR-2 localizes to the posterior cortex, but the microtubule-binding mutant R183-5A and the RING mutant C56S do not. Endogenous PAR-2 [PAR-2(+)] rescues the localization of both mutants. Rescue is also observed in *par-1* zygotes, where PAR-3 and PKC-3 are never excluded from the posterior cortex (see Fig. 4a).

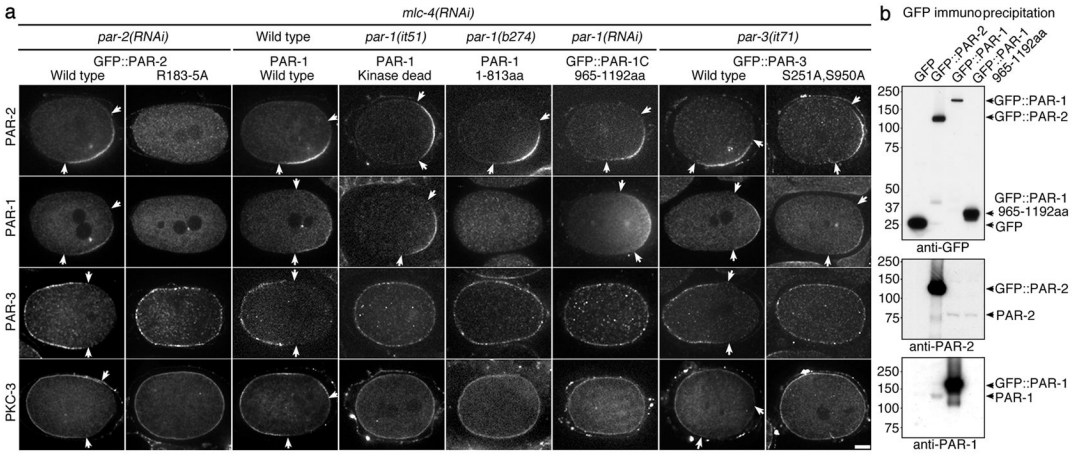

Figure 4. PAR-2 recruits PAR-1 to the cortex, leading to exclusion of anterior PARs

(**a**) *mlc-4(RNAi)* zygotes with indicated mutations in PAR proteins stained for PAR-2, PAR-1, PAR-3 and PKC-3. *par-1(it51)* contains a mutation (R409K) that inhibits kinase activity[14], and *par-1(b274)* contains a premature stop (Q814Stop) that eliminates the PAR-1 cortical localization domain[15]. GFP::PAR-3(S251A S950A) contains mutations in the conserved PAR-1 phosphorylation sites and rescues *par-3(it71)* zygotes competent for cortical flows[16]. GFP::PAR-2 fusions were co-stained with PAR-1. PAR-2 and PKC-3 or PAR-1 and PAR-3 were co-stained in the other zygotes. Arrows indicate the boundary of the PAR domains. Scale bar, 10 μm.

(**b**) Immunoprecipitation experiment showing that PAR-2 and PAR-1 interact in embryo extracts. Extracts from embryos expressing the indicated GFP fusions were immunoprecipitated with anti-GFP-beads and the immunoprecipitates were blotted with the indicated antibodies.

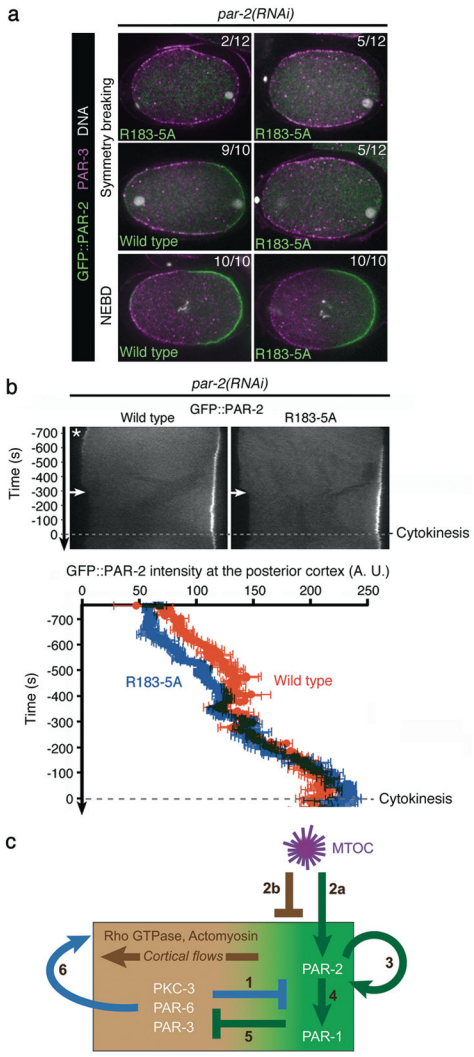

Figure 5. Microtubule binding by PAR-2 is required for efficient polarity initiation in wild-type embryos

(**a**) Fluorescent micrographs of fixed zygotes expressing GFP::PAR-2 and depleted for endogenous PAR-2 by RNAi. Zygotes are stained for GFP::PAR-2 (green), PAR-3 (magenta), and DNA (white) and shown at symmetry breaking (first two rows) or at NEBD (last row). Scale bar, 10 μm.

(**b**) Kymographs from time-lapse movies of live zygotes expressing GFP::PAR-2 fusions and depleted for endogenous PAR-2 by RNAi. Times are with respect to the onset of cytokinesis. Wild-type GFP::PAR-2 appears on the posterior cortex earlier than the microtubule-binding mutant GFP::PAR-2(R183-5A). Wild-type GFP::PAR-2 also accumulates transiently (asterisk) on the anterior cortex (due to the transient influence of the meiotic spindle remnant[18]; 5 of 5 zygotes). GFP::PAR-2(R183-5A) does not show this localization (0 of 5), consistent with polarization by the meiotic spindle depending primarily on microtubules[7]. Graph shows fluorescence intensity at posterior most cortex averaged from five zygotes. Accumulation of GFP::PAR-2(R183-5A) is delayed compared to wild-

type GFP::PAR-2 (29.0 +/− 11.2 seconds, p=0.03) but catches up by NEBD. Error bars represent standard deviation from five separate zygotes.

(**c**) Model for polarization of the *C. elegans* zygote

1) PKC-3 phosphorylates PAR-2[12] and PAR-1, keeping them off the cortex.

2) MTOC breaks symmetry via two parallel mechanisms: **2a**; Microtubules at the MTOC protect PAR-2 from phosphorylation by PKC-3, allowing a few molecules of PAR-2 to load on cortex close to MTOC. **2b**; MTOC induces cortical flows by an unknown mechanism involving local inhibition of actomyosin[3]. Flows displace anterior PARs, allowing PAR-2 to accumulate in their place.

3) Cortical PAR-2 recruits additional PAR-2 molecules to expand the PAR-2 domain. RING finger of PAR-2 stabilizes PAR-2 at the cortex.

4) PAR-2 recruits PAR-1 by binding to the C-terminus of PAR-1.

5) PAR-1 phosphorylates PAR-3 preventing its association with the cortex.

6) Anterior PARs stimulate their own displacement by recruiting myosin to the cortex and up-regulating cortical flows[3, 4].

Not shown in this figure is LGL, a non-essential player in this process, which like PAR-1 localizes to the posterior cortex and antagonizes the cortical association of anterior PARs[24, 25].